

## CHARACTERIZATION OF DUCTILE TEARING RESISTANCE BY ENERGY DISSIPATION RATE

D. Memhard<sup>1</sup>, W. Brocks<sup>1</sup>, S. Fricke<sup>2</sup>

The concept of energy dissipation rate as proposed by Turner is discussed to provide a better understanding of ductile tearing. It is shown how this quantity can be calculated in a finite element analysis, or re-evaluated from J-R test records of bend and tensile specimens. The energy dissipation rate is decreasing with crack extension in gross plasticity and approaches a stationary value. It depends on specimen size and loading type, too, but the different curves can be scaled by a simple normalization based on limit analysis.

The shapes of the cumulative J-R curves can be derived for different specimen geometries. Thus, a quantitative explanation of geometry dependence of R-curves is given.

INTRODUCTION

Ductile tearing resistance of a material is conventionally characterized by a J-resistance curve which is obtained from bend-type specimens, i.e. C(T) or SE(B), by standard procedures [1]. It characterizes, within certain limits set forth in the standards, the resistance against slow stable crack growth. These limits are severe. First of all, J-R curves refer to bending configurations only, and it is well known [2,3] that they will be different, e.g., for tensile loading and generally depend on the specimen geometry and loading configuration. Second, the standards require that the permitted crack extension does not exceed one tenth of the remaining ligament. These requirements may inhibit the application to structural components in many cases when large crack extension and fast ductile fracture have to be considered or when the loading configuration is closer to tension.

Klemm [4] introduced a parameter called crack propagation energy, which is the

---

<sup>1</sup> Fraunhofer-Institut für Werkstoffmechanik Freiburg, Germany

<sup>2</sup> Technische Universität Berlin, Germany

dissipated energy,  $dU_{dis}$ , per increment of crack area,  $dA$ ,

$$R = \frac{dU_{dis}}{dA} \quad (1)$$

to characterize the material resistance against fast ductile fracture in pipeline steels. This definition is a straight transfer of Griffith's elastic energy release rate to plastic processes which is consistent with the incremental theory of plasticity. In fact, the cumulative quantity  $J$ , which rises with increasing crack length, is not the true driving force for ductile tearing as Turner [5] has pointed out in a basic discussion on the necessity of defining an alternative measure of tearing toughness. He proposed to define tearing resistance in terms of energy dissipation rate. Although both approaches have been proposed independently for different cases of applications they both come to the same definition, eqn. (1).

The present contribution intends to give further evidence to this concept. Procedures to measure or calculate  $R$  are described and discussed and it will be shown that  $R$  approaches a stationary value after a transition phase. This stationary value,  $R_{\infty}$ , depends on the hardening properties of the material but also on the loading configuration, tension or bending, and the size of the plastic zone. An example is given how specimen dependent  $R(\Delta a)$  curves can be scaled by a normalizing factor obtained from a plastic limit analysis. The J-R curves for bend- and tensile-type specimens and for large stationary crack extension beyond the limitations of current test standards and available test data can be obtained analytically by integrating the respective differential equations and introducing an exponential regression function for  $R(\Delta a)$ .

#### DEFINITION AND EVALUATION OF $R$

Since Griffith's considerations on rupture in solids the "energy approach" to fracture phenomena has become one of two supporting legs of fracture mechanics. It is based on the material independent law of conservation of energy which is written down for an incremental process between times  $t$  and  $t+\Delta t$  involving a crack extension of area  $\Delta A = \dot{A} \Delta t$ . The main difficulty in elastic-plastic fracture mechanics consists in separation of the two dissipative terms in the balance of power, i.e. the rates of plastic work,  $\dot{U}_{pl}$ , and "fracture energy",  $D_f \dot{A}$ . Such separation would be necessary in order to formulate a relevant fracture criterion, since  $\dot{U}_{pl}$  is not a material constant but depends on geometry and loading conditions. In the R-curve method, the difference between the two terms is not recognized leading to a number of inconsistencies well known as "constraint effects". Kolednik [6] gave obvious examples what  $J$ - $\Delta a$  curves really mean in gross plasticity. Many attempts have been made to split the dissipated energy into (local) fracture energy and (global) plastic energy, but did not yet yield

satisfactory results. Turner [5] doubts that splitting dissipation into fracture and plasticity is possible at all. He suggests the combined plastic plus fracture dissipation rate to be more relevant and fundamental to plastic tearing than any quantity derived from total work. At least, a rate quantity is consistent with the basic idea of incremental theory that plastic processes can only be described by rate equations, whereas "total" quantities follow by integration and depend on the integration path.

For quasi-static processes,  $R$  can be simply evaluated from the area under the load vs. displacement curve by

$$R = \frac{dU_{pl}}{dA} + D_f = \frac{dW_{ex} - dU_{el}}{dA} \quad (2)$$

where  $W_{ex}$  is the work done by external forces and  $U_{el}$  is the elastic energy of the body. In this definition  $R$  includes the whole irreversible part of the work done and, hence may also include plastic work in zones far remote from the crack tip, e.g. around load points or supports. If an elastic-plastic finite element (FE) analysis of crack growth [7] is performed, the rate of plastic work can be calculated directly from stresses and strains

$$\dot{U}_{pl} = \int_V \sigma_{ij} \dot{\epsilon}_{ij}^{pl} dV = \int_V \sigma_e \dot{\epsilon}_e^{pl} dV \quad (3)$$

$\sigma_e$  and  $\epsilon_e^{pl}$  being von Mises effective stress and effective plastic strain, respectively. Since the FE model basing on the Mises-Prandtl-Reuss constitutive equations reflects plastic processes, only, we have  $R = dU_{pl} / dA$ .

#### DISSIPATION RATE $R$ AND CUMULATIVE QUANTITY $J$

The standard procedures of evaluating  $J$  from single specimen test data use recurrence formula to account for the change in crack length. These formula split the total  $J$  into an elastic and a plastic component and sum up the increments of area under the non-linear load vs. displacement curve for the second component [1]. In fact, these increments represent dissipated work per crack length increment, though they are characterized as "plastic". The recurrence formula can easily be used to re-evaluate the dissipation rate of eqn. (2) from J-R test data. Memhard and Klemm [8] have derived the relation for C(T) and SE(B) specimens

$$R = \frac{W-a}{\eta} \frac{dJ_{pl}}{da} + J_{pl} \frac{\gamma}{\eta} \quad (4)$$

from the J-formula used in ASTM E 1152 [1] with  $\eta(a/W)$  and  $\gamma(a/W)$  being

geometry functions. Similarly, the relation

$$R = (W - a) \frac{dJ_{pl}}{da} \quad (5)$$

is obtained for M(T) specimens using the J-formula of Schwalbe and Hellmann [9] which was derived from considerations by Garwood, Robinson and Turner [10]. These equations allow one to re-evaluate the energy dissipation rate from J-R test data. They show that the dissipation rate,  $R$ , is converted into  $J$  differently for bend-type and tensile type specimens. This means that resulting J-R curves must necessarily be different for a C(T) and a M(T) specimen. Generally, if the function  $R(\Delta a)$  is known, the differential eqns. (4) and (5) for  $J_{pl}$  can be solved and the shape of the corresponding J-R curve will be obtained.

Generally, the decaying shapes of the  $R(\Delta a)$  curves can be fitted by three parameters with an exponential curve [11]

$$R = R_{\infty} [1 + \alpha e^{-\lambda a/W}] \quad (6)$$

Here  $\lambda$  governs the intensity of decay from the initial value,  $R_0 = R(a_0)$ , to the steady-state value,  $R_{\infty}$ , and  $\alpha$  defines the initial value,  $R_0$ . The term  $R_{\infty}$  is the "crack propagation energy" for steady state growth. The differential equations for  $J_{pl}$ , eqs. (4) and (5), can then be solved analytically and closed form expressions for J-R curves of tensile and bend specimens are obtained [11].

#### CRACK GROWTH IN C(T) AND M(T) SPECIMENS

R-curve test data from compact specimens, C(T), and centre cracked tensile panels, M(T), made of the German standard steel StE 460 were used for numerical crack growth simulations which followed the respective experimental  $J(\Delta a)$  curves, Fig. 1. All specimens were side grooved, had a width of  $W = 50 \text{ mm}$ , a net thickness of  $B_n = 20 \text{ mm}$  and  $16 \text{ mm}$ , and a crack length ratio of  $a_0/W = 0.5$  and  $0.6$  for C(T) and M(T), respectively. The specimens have been tested up to 6 to 8 mm crack growth beyond the accepted limits of "J-control" [1] in order to investigate "geometry effects" for large ductile crack growth [12]. All specimens were fully yielded at initiation of crack growth. The FE models were two-dimensional, assuming plane strain conditions, and subject to prescribed displacements. The global displacements in load direction,  $V_L$ , plotted vs. crack extension,  $\Delta a$ , show a qualitatively similar behaviour for both specimen geometries, Fig. 2, whereas the load vs. displacement curves in Figs. 3 and 4 look quite different. The net thickness  $B_n$  was used for calculating the total force for the FE model in order to compare with the test data.

Fig. 5 shows the growth of the plastic zone size,  $A_{pl}$ , with crack growth,  $\Delta a$ , for both specimen geometries. Only the plastic zone around *one* crack tip is plotted which means one half of the total value for the M(T) specimen. Whereas the plastically deformed area in the C(T) specimen does not change remarkably, it increases after initiation in the M(T) specimen up to almost double size and remains approximately constant after 2 mm crack growth. For both specimens, the steady state value of  $A_{pl}$  is reached at load maximum, but it is about four times larger for the tensile-type compared with the bend-type specimen. Though the plastic zone size remains constant the dissipated plastic work keeps increasing, see Fig. 6. It can either be calculated from global quantities, i.e. the area under the load vs. displacement curves, Figs. 3 and 4, or from local quantities, eqn. (3). Again, only the deformation energy dissipated in *one* plastic zone was evaluated for the M(T) specimen. Yet,  $U_{pl}$  is up to eight times greater in the M(T) than in the C(T) which is due, first, to the larger plastic zone and, second, to higher plastic strains.

Whereas the total plastic work is continuously increasing, the dissipation rate,  $R$ , calculated from either eqns. (2), (3), or (4) and (5), respectively, is decreasing and approaching a stationary value for large crack growth as is shown in Figs. 7 and 8. It is about ten times greater for the centre cracked specimen. In other words, as ductile crack propagation consumes ten times as much work, the centre cracked specimen has the higher "tearing resistance". The latter also behaves more stably than the compact specimen, which can be noticed in the load vs. displacement curves of the two structures, Figs. 3 and 4. If the regression curves, eqn. (6), of  $dU_{pl} / Bda$ , obtained from the evaluation of eqn. (3), are integrated according to the solutions of the differential equations (4) and (5), respectively, which are given in [11], a good agreement is obtained with the experimental J-R curves, see Fig. 9. Of course, this is not a surprising result but just a verification of the derived formulas. However, it may elucidate the true nature of J-R curves once more, and the fact that they can never be expected to be geometry independent.

#### NORMALIZED CRACK PROPAGATION ENERGY

The quantity  $R$  is dependent on the plastic zone size and the kind of loading too, see Figs. 7 and 8, and thus it does not help directly in solving the problem how to transfer test results from specimens to large scale components. But one can try to normalize it appropriately. The obvious idea to convert the dissipation rates of two structures by the ratio of their respective plastic zone sizes does not work, as Fig. 10 shows. As crack initiation and growth occurs under fully plastic conditions, the plastic limit load of the specimens might be an appropriate scaling factor.

A lower bound analysis yields

$$\frac{F_{pl}^{low}}{B(W-a_0)\sigma_f} = \begin{cases} \frac{\sqrt{2(W^2+a_0^2)} - (W+a_0)}{W-a_0} & \text{for C(T)} \\ 2 & \text{for M(T)} \end{cases} \quad (7)$$

For hardening materials the "flow" stress is commonly assumed as  $\sigma_f = \frac{1}{2}(\sigma_y + \sigma_u)$ . The real limit load is greater or equal the lower bound

$$F_{pl} = \kappa_{pl} F_{pl}^{low} \quad \text{with} \quad \kappa_{pl} \geq 1 \quad (8)$$

If we take the ultimate load,  $F_u$ , from Figs. 2 and 3 we obtain  $\kappa_{pl} = 1.55$  for the C(T) and  $\kappa_{pl} = 1.20$  for the M(T) specimen, respectively. An upper bound of the limit load can be found from slip line theory and the limit load estimated from upper and lower bounds if no experimental data are available. Fig. 11 shows the energy dissipation rate normalized by the respective dimensionless limit load factor,  $F_u / B(W-a_0)\sigma_f$ . The normalized steady state crack propagation energy appears to be the same for both specimen geometries. The normalization does not work well for the beginning ( $\Delta a < 2$  mm) where the plastic zone size of the M(T) specimen is still increasing, see Fig. 5.

### CONCLUSIONS

The dissipation rate  $R$  is a physically more meaningful quantity for describing the ductile tearing resistance of a structure than the conventionally used  $J$  integral. It measures the increment of external work which is necessary to propagate the crack by some amount,  $\Delta a$ , whereas  $J$  accumulates the plastic work done along a given loading path. Whereas J-R curves keep rising even for steady state crack extension,  $R$  decreases with  $\Delta a$  and approaches a stationary value,  $R_\infty$ .

J-R curves can be derived analytically from  $R(\Delta a)$  curves by integrating the respective differential equations for bend- and tensile-type specimens. This allows to extrapolate J-R curves for large stationary crack extensions beyond the limitations of current test standards and even beyond available test data.

Obviously,  $R$  depends on the geometry and the type of loading of the specimen or the structure. It can therefore not be transferred from a specimen to a component in a straightforward way, but neither can  $J$ . It has been shown for a C(T) and a M(T) specimen that this geometry dependence can be scaled by a limit load factor. There is no general evidence that this scaling will work for other geometries and materials. No answer can yet be given, either, as to whether or not

this concept applies to real three dimensional configurations. But it seems that one step forward has been done in understanding and quantifying "geometry dependence" of R-curves. As  $R(\Delta a)$  curves can be easily re-evaluated from existing J-R test records, it seems worthwhile to try to verify the normalization procedure for further cases.

## REFERENCES

- [1] ASTM E 1152-87, "Standard test method for determining J-R curves", Annual Book of ASTM standards, Vol. 03.01, American Society for Testing and Materials, Philadelphia.
- [2] Garwood, S.J., "Effect of specimen geometry on crack growth resistance", ASTM STP 677, 1979, pp. 511-532.
- [3] Link, R.E., Landes, J.D., Herrera, R. and Zhou, Z., "Defect Assessment in Components, Fundamentals and Applications", Edited by J.G. Blauel and K.-H. Schwalbe, ESIS/EGF 9, Mechanical Engineering Publications, London, 1991, pp. 707-721.
- [4] Klemm, W. (1989): "Dynamic Fracture Mechanics for the 1990s", Edited by H. Homma, D.A. Shockey and G. Yagawa, Proc. of the 1989 ASME Pressure Vessels and Piping Conference, pp. 99-104.
- [5] Turner, C.E., "Fracture Behaviour and Design of Materials and Structures", Edited by D. Firrao, Proc. 8th European Conference on Fracture, Engineering Materials Advisory Service, Warley, UK, 1990, Vol. II, pp. 933-949, 951-968.
- [6] Kolednik, O., Engineering Fracture Mechanics, Vol. 38, 1991, pp. 403-412.
- [7] Siegele, D. and Schmitt, W., Computers & Structures, Vol. 17, 1983, pp. 697-703.
- [8] Memhard, D. and Klemm, W., Proc. 24th Meeting of DVM Working Party on Fracture Events, Berlin, German Association for Materials Research and Testing, 1992, pp. 291-302.
- [9] Schwalbe, K.-H. and Hellmann, D., "Correlation of stable crack growth with the J-integral and the crack tip opening displacement, effects of geometry, size, and material", Report GKSS 84/E/37, GKSS-Forschungszentrum Geesthacht, 1984.
- [10] Garwood, S.J., Robinson, J.N., and Turner, C.E., Int. J. of Fracture, Vol. 11, 1975, pp. 528-530.
- [11] Memhard, D., Brocks, W., and Fricke, S., Fatigue Fract. of Engng. Mater. Struct., Vol. 16, 1993, pp. 1109-1124.
- [12] Aurich, D. et al., "Analyse und Weiterentwicklung bruchmechanischer Versagenskonzepte", Research Report BAM 174, Federal Institute for Materials Research and Testing, Berlin, 1990, pp.15-60.

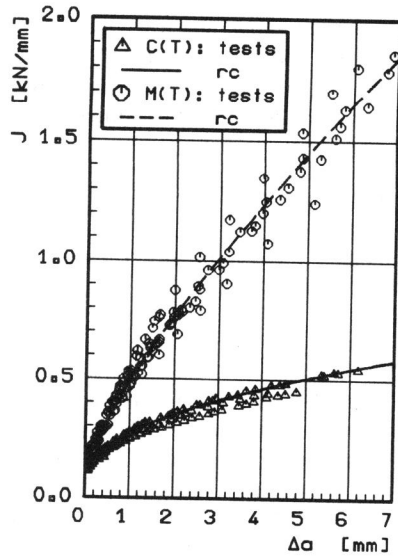


Fig. 1:  $J_R$  curves of steel StE 460, test results and regression curves (rc)

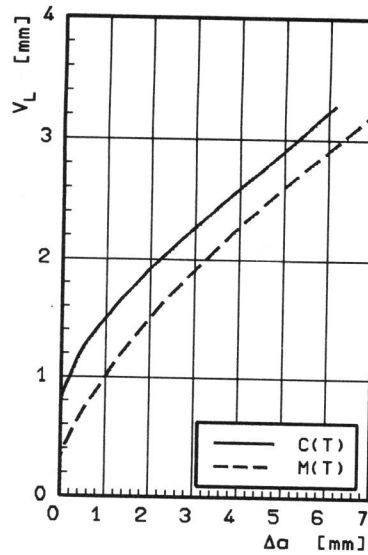


Fig. 2: Displacements in loading direction from FE analysis

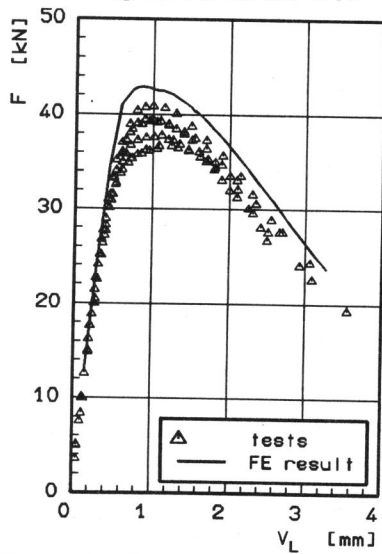


Fig. 3: Load vs crack opening of C(T), test results and FE analysis

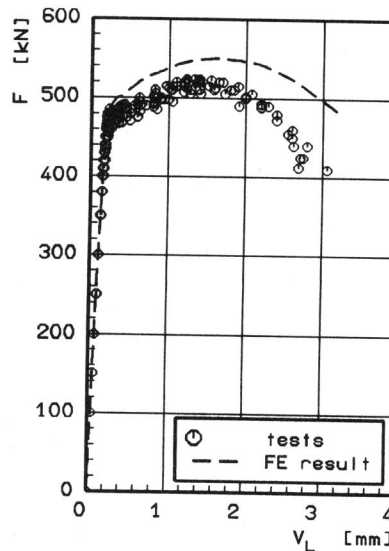


Fig. 4: Load vs elongation of M(T), test results and FE analysis



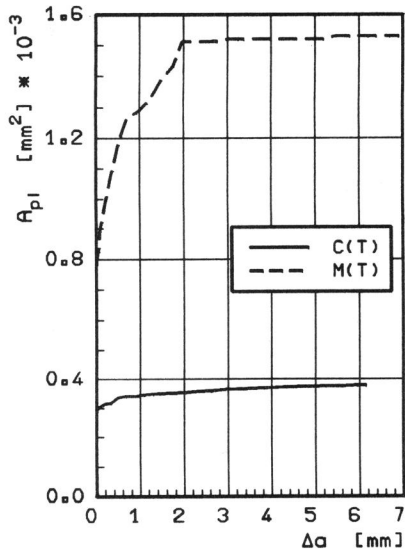


Fig. 5: Plastic zone size from FE analysis

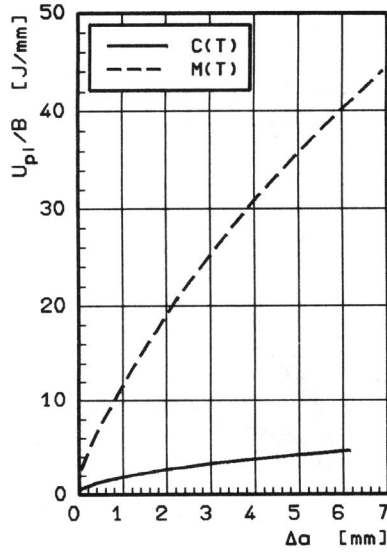


Fig. 6: Dissipated deformation energy

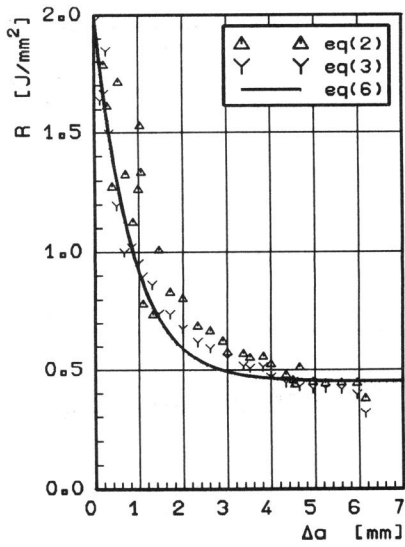


Fig. 7: Dissipation rate R for C(T), global and local evaluation

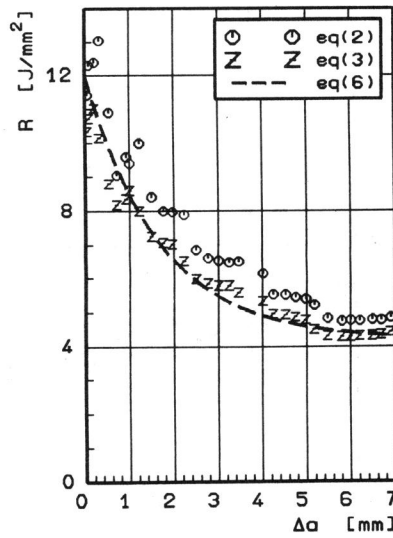


Fig. 8: Dissipation rate R for M(T), global and local evaluation

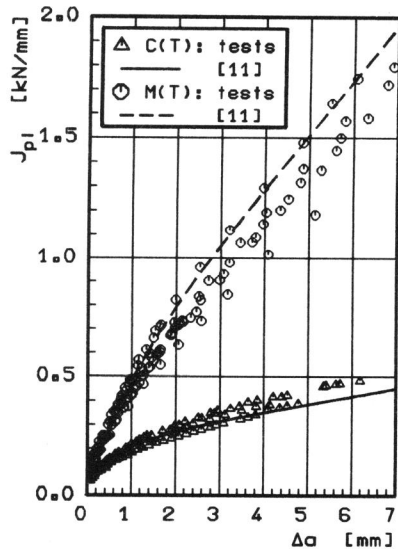


Fig. 9:  $J_p$  curves for C(T) and M(T), test results and integration of  $R(\Delta a)$  [11]

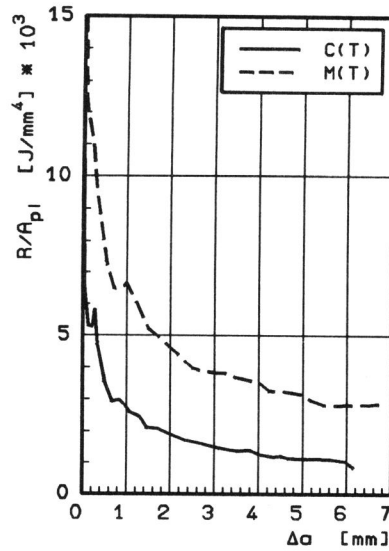


Fig. 10: Dissipation rate  $R$  normalized by plastic zone size

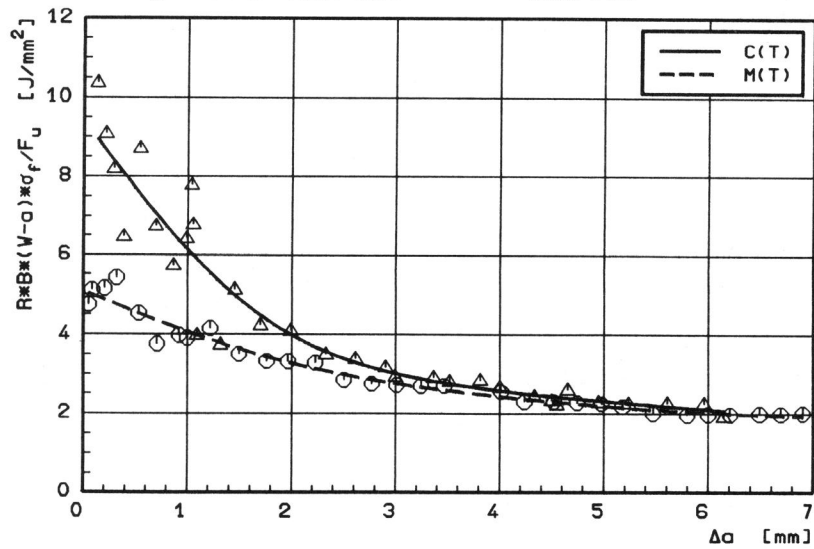


Fig. 11: Dissipation rate  $R$  normalized by limit load factor